Specificity, flexibility and valence of DNA bonds guide emulsion architecture

Lang Feng[1+], Lea-Laetitia Pontani[1+], Rémi Dreyfus[2], Paul Chaikin[1], Jasna Brujic[1*]

[1]Center for Soft Matter Research and Department of Physics, New York University, New York, New York, 10003

[2]Complex Assemblies of Soft Matter Laboratory, CNRS/Rhodia/UPenn UMI 3254, 350 Georges Patterson Boulevard, Bristol, PA, 19007, USA

[+]These authors contribute equally to this work

[*]Corresponding Author, E-Mail: jb2929@nyu.edu

The specificity and thermal reversibility of DNA interactions[1] have enabled the self-assembly of crystal structures[2-8], self-replicating materials[9,10] and colloidal molecules[11]. Grafting DNA onto liquid interfaces of emulsions[12] leads to exciting new architectural possibilities due to the mobility of the DNA ligands and the patches they form between bound droplets. Here we show that the size and number of these adhesion patches (valency) can be controlled. Valence 2 leads to flexible polymers of emulsion droplets, while valence above 4 leads to rigid droplet networks. A simple thermodynamic model quantitatively describes the increase in the patch size with droplet radii, DNA concentration and the stiffness of the tether to the sticky-end. The patches are formed between droplets with complementary DNA strands or alternatively with complementary colloidal nanoparticles to mediate DNA binding between droplets. This emulsion system opens the route to directed self-assembly of more complex structures through distinct DNA bonds with varying strengths and controlled valence and flexibility.

Self-assembly of particles is of great interest for the design of complex particulate architectures to create smart nano-materials with tunable optical [13], mechanical

[14] or electronic properties [15,16]. The specific and programmable interaction between complementary DNA strands is a good candidate for self-assembly [4,5,17,18]. Combining short DNA sequences with soft matter has led to diverse assemblies [2-10,17]. Most recently, DNA binding was used to assemble colloidal molecules with specific symmetries imposed by the positions of the grafted DNA [11]. Enabling the DNA to diffuse freely on the surface of emulsion droplets [12] allows the system to explore configurations in the underlying free energy landscape. To this end, we have grafted DNA strands onto thermal oil-in-water emulsions [19]. Mixing two emulsions with complementary DNA strands leads to their specific binding through strong yet reversible adhesion patches. Unlike solid colloidal particles, liquid droplets are able to rearrange within the packed structure once they are bound together. Moreover, the deformation of the emulsion droplets, i.e. the size of the adhesion patch, provides a direct probe of the free energy of binding. We develop a thermodynamic model to relate the adhesion size to the binding free energy and discover that the entropy loss upon binding plays an important role. We test the validity of the model by varying the DNA surface density, the stiffness of the tether and the droplet size. This system therefore sheds light on the mechanisms of adhesion between contacting liquid surfaces. Emulsion self-assembly leads to segregated floppy networks, which are amorphous materials with interesting rheological properties. In addition, we show that colloidal nanoparticles can serve as mediators of the DNA interaction between droplets. Controlling their concentration determines the valence of the droplets and enables us to uniquely create linear emulsion strings or those that fold into compact clusters. Consequently, this system represents a powerful tool for self-assembly applications [20-25].

The model emulsion system in Fig. 1A is stabilized with a mixture of two phospholipids, Egg-Phosphatidylcholine (EPC) and PEG-biotinylated lipids, and a small amount of SDS surfactant, as described in [19]. The biotinylated lipids are saturated with fluorescent streptavidin, which in turn binds to a second biotin from the functional DNA strand. The green emulsion (Alexa Fluor 488® streptavidin) is coated with the S sequence, while the red emulsion (Alexa Fluor 633® streptavidin) is coated with the S' sequence (see Materials and Methods). In addition to the complementary sticky ends, the binders have an identical backbone of either single stranded or double stranded DNA that serves as a tether to the binder. Alternatively, we study a hybrid system of interacting colloidal nanoparticles and emulsions, as illustrated in Fig. 1B. In this system the emulsion is only decorated with the S' DNA sequence (red), which interacts with colloids coated with the complementary S sequence (green). As a result, a colloidal particle binds droplets together.

The thermal reversibility of DNA interactions in these systems [6,10,17,22] allows us to switch the adhesion between droplets on and off by cycling the temperature above and below the DNA melting temperature of T_m=50°C. At room temperature, complementary emulsions are mixed together and diffuse to form adhesive clusters (Fig. 1C left panel) that dissociate upon heating above T_m (Fig. 1C right panel and Supplementary Movie). Similarly, the emulsion-colloid system below Tm reveals multivalent particle-emulsion structures (Fig. 1D left panel) that are separated upon heating (Fig. 1D right panel).

When complementary droplets meet, their DNA strands hybridize to form double-stranded (ds) DNA. Therefore, the presence of green and red streptavidin, associated with each DNA strand, lead to yellow adhesion patches in regions of

hybridization, as shown in Figs. 2A (dsb) and 2B (ssb). Interestingly, the patches in emulsions with double stranded backbone (dsb) tethers are significantly larger than those with single stranded backbone (ssb) tethers. In both cases, the plot of the patch size as a function of the reduced radius of each pair of contacting droplets in Fig. 2C reveals a linear dependence. Thus, the measured ratio of dsb to ssb patch sizes of ~1.6 is independent of droplet size. This result implies that the strength of binding between droplets can be modulated *in situ* by adding the complementary strand to ssb functionalized emulsions. Indeed, we observe that the patch size transitions from the average size expected for ssb DNA interactions to the ~1.6 times larger adhesions corresponding to dsb DNA in less than one hour, as shown in Fig. 2D.

Another way to increase the binding strength, as well as the number of patches per droplet, is to increase the DNA coverage on the droplets, C_α, as shown in the 3D images in Fig. 3A. The patch size (θ) and the relative intensity, defined as the ratio of the intensity of fluorescence in the patch and that of the droplet surface, increase as a function of DNA coverage in Figs. 3B and C. This capability allows one to tune the reversibility of droplet interactions and the temperature at which the structures melt.

These experimental observations are explained by a statistical mechanical model. The model is based on the assumption that binders are recruited into the contact area until the binding energy balances the energy cost upon droplet deformation and the entropy penalty due to the immobilization of the DNA tether in the patch. Let us consider two complementary emulsion droplets with the same radius R_e and DNA surface density $N_0/(4\pi R_e^2)$, where N_0 is the total number of DNA on the droplet. The two droplets interact to form an adhesive patch of radius r_p and deformation

angle $\theta=r_p/R$, as shown in Fig. 1A. We note N_β the number of DNA binders inside the patch between two complementary droplets, and N_α the amount of free DNA strands remaining on the droplet surface. The global free energy change from the unbound to the bound state is then:

$$\Delta F= \Delta E_{DNA,\beta} -2T(S_\beta+S_\alpha)+E_{deform}- F_{unbound} \quad (1)$$

where E_{dna} is the binding energy, T is the temperature, S is the entropy of binding and E_{deform} is the energy cost to deform the interface. Subscripts β and α indicate the binding patch region and the unbound surface, respectively. In the dilute case, $S_\beta=-kN_\beta \ln[C_\beta/C_0]$ where $C_\beta=N_\beta/\pi r_p^2$ is the surface density of DNA in the adhesive patch and C_0 is the reference concentration, which cancels out in the calculation. The binding free energy for the mobile DNA patch is estimated in mean field: $\Delta E_{DNA,\beta}=N_\beta[\Delta G_{DNA}-T\Delta S_r-k_BT \ln(A_wC_\beta)]$, where ΔG_{DNA} is the free energy of hybridization of free DNA in solution, ΔS_r is the entropy loss due to rotational constraints of hybridized DNA strands at low temperature [22,23], A_w is the area in which two DNA strands can move relative to each other when hybridized and $\ln(A_wC_\beta)$ is the translational entropy penalty for two DNA strands bound in the patch. The deformation energy is given by $E_{deform}=\sigma\pi R_e^2\theta^4/2$, where σ is the surface tension [19]. Since there are only two independent parameters in the problem, C_β and r_p, we minimize the global energy to obtain the profile of $C_\beta(C_\alpha , A_w)$ and $\theta(C_\alpha, , A_w)$:

$$\theta(C_\alpha, , A_w) = r_p/R_e=\left[\frac{kT[-2\ln\left(1-C_\beta A_{strep}\right)-C_\beta A_{strep}]}{\sigma A_{strep}}\right]^{1/2} \quad (2)$$

assuming that the binding free energy ΔG_{DNA}, the surface tension σ, the streptavidin size A_{strep} and the temperature T are kept constant (see Supplementary Information for details).

Since the double stranded tether is much longer and can reach as far as ~26nm [22], further than that of the single stranded tether of ~4.5nm [26], the area of relative motion of bound DNA strands, A_w, is also much larger, estimated to be ~2000nm^2 compared to only ~60nm^2. Therefore, the dsb case loses less entropy upon binding (see [22][23] and Supplementary Information), which quantitatively explains the ~1.6 fold larger average patch size, as shown in Fig. 2C. Moreover, we capture the adhesion strength dependence on the DNA surface coverage with only 2 fitting parameters: the rotational entropy loss ΔS_r=-16R (where R is the gas constant) and the maximum DNA binding capability, N=12pmol, for an emulsion sample of 30μL. These fitting parameters are consistent with previously reported values [19, 22, 23] (see Supplementary Information). The agreement of the model with the experimental data for the three trends shown in Fig. 2C and Fig. 3B-C gives validity to our theoretical framework.

The fluidity of the droplet surface enables rearrangements in bound structures and allows for the self-assembly of programmable geometries. Adhesion patches are free to diffuse despite the high binding energy of ~20000 DNA connections in an average-sized patch with a 1.6μm diameter. Figure 4A shows the diffusion of droplets that are bound through DNA interactions, but free to rotate with respect to each other and thus explore available configurations. We use hybrid systems of particles and emulsions to quantify the diffusion of adhesion patches (Fig. 4B). The beads serve as reporters for the lipid motion on the monolayer surface. To measure relative motion, two colloidal particles coated with the S DNA sequence are attached onto the surface of a S' functionalized droplet through at least 200 DNA bonds [22,23]. The mean square displacement of one bead with respect to the other (graph in Fig. 4B) yields a diffusion constant of D~0.012 μm^2/s. This value is significantly smaller than both the diffusion of a single lipid of size ~1nm in a fluid model

membrane with D~1-10 $\mu m^2/s$ [27-30] and that of a 1 μm colloidal particle with $D_{particle}$~0.5 $\mu m^2/s$. This slow diffusion of the particle is due to the strong hydrodynamic drag of an adhesive lipid patch of radius ~100nm [22], which is expected to be two orders of magnitude lower than that of a single lipid [29,30].

Allowing the emulsions to cream to the surface assembles floppy networks of bound droplets that are organized by the specificity of the DNA bonds, as shown in Fig. 4C and Supplementary Information. Once the maximum droplet connectivity is achieved, no further rearrangements in the structure are observed. Nevertheless, the bonds continue to be mobile owing to the liquid interfaces. While the coordination number distribution of such networks can be tuned by the concentration of binders on the surface, their structure remains amorphous.

Alternatively, the complementary colloid-emulsion hybrid system, shown in Fig. 1B, is a versatile tool for self and directed-assembly. Combining the dilute emulsion (~1000 droplets/mm^2) with complementary nanoparticles at a low particle/droplet ratio of ~5 enables the formation of linear emulsion polymers of different lengths, as shown in Fig. 5A. The linear arrangement of the droplets is induced by constraining them in a 1-D line at the edge of a tilted rectangular capillary (see Supplementary Information). The binding colloids are recruited exclusively to the emulsion contacts after overnight incubation to form two patches per emulsion droplet and thus prevent branching. This leads to polymer chains with a valency of 2 that diffuse over time due to the mobility of the particulate joints between the droplets. They remain in a linear configuration because the particles are too small to bridge three droplets. On the other hand, at a higher particle/droplet ratio of ~100 we observe multivalency and folding of the linear chains into compact structures over time, as shown in Fig. 5B. In that case, the

binding energy of the multivalent particles and their connectivity is sufficient to arrest the resulting structure. The geometry of the final compact structure depends on the valency, the number of droplets in the cluster, as well as the kinetic pathway, and ranges from triangular lattices to flowers, as shown in Fig. 5C. These structures lower their energy by maximizing the number of colloids that occupy emulsion contacts. Unlike droplet-droplet patches, shown in Figs. 2,3 and 4, the solid polystyrene particles are large enough to bridge two emulsion droplets without reaching their contact point. This leads to a ring structure in the adhesion zone, as shown in the confocal images of clusters in Fig. 5D (see also Supplementary Movie). The circular arrangement maximizes the number of particles per emulsion contact and thereby minimizes the global free energy.

We have achieved the self-assembly of thermal emulsion polymer chains with programmable droplet interactions. Controlling the number of binders and the length of the chain we obtain divalent, trivalent and multivalent structures. In addition, the mobility of adhesive patches within these structures allows them to evolve into geometries that are governed by the underlying free energy landscape. Furthermore, DNA interactions allow one to program the shape of the free energy landscape through the control of bond specificity, strength, flexibility and valency. This system promises to become the gold standard in directed self-assembly because it has the potential of building intelligently designed materials, such as colloidal crystals or artificial self-replicating materials, with no external inputs.

Methods:

Synthesis of biomimetic emulsion: The protocol for the emulsion preparation is described in [19]. The oil droplets are stabilized with egg L-α-phosphatidylcholine (EPC) lipids and the DSPE-PEG(2000) biotinylated lipids from Avanti Polar Lipids at

a molar ratio of 92:8, respectively. After cooling to room temperature the lipid containing oil (10 mL) can be emulsified in two different buffers to reach different droplet sizes. Athermal droplets are obtained when emulsified in a buffer containing 5mMSDS and w_t=18% dextran and sheared at 22rpm in the narrow gap couette mixer. Smaller droplets sizes are obtained with a buffer containing 5mMSDS and w_t=4.5% alginate and a shearing rate of 30rpm. The resulting emulsions are stable over several weeks at 4 °C.

DNA coated emulsion preparation: The emulsion is first coated with two different fluorescent streptavidins: Alexa Fluor 488® and Alexa Fluor 633® streptavidin (Molecular Probes). 100µL of emulsion is mixed with 10 µL of 1mg/mL streptavidin and 300 µL of buffer containing 2mM Tris pH=7 and 1mM SDS. The solution is incubated 1h at 4 °C and then washed twice with the same buffer, before a final wash in the DNA buffer (1mM SDS, 5mM PBS, 4mM $MgCl_2$). The DNA can then be added to the streptavidin coated emulsion: 10 µL of 50µM DNA is added to the solution and incubated 1h at room temperature. The remaining unbound DNA is finally washed three times in the DNA buffer. One type of fluorescent streptavidin is specifically associated with one DNA strand in order to distinguish them by microscopy.

DNA constructs:

The S strand has a sequence: 5'-BiotinTEG-49bp backbone-GGATGAAGATG-3';

The S' strand has a sequence:5' -BiotinTEG-49bp backbone-CATCTTCATCC-3';

The CS strand complementary to the backbone: 5'-TCG TAA TGA AAG GCA GGG CTC TCT GGA TTG ACT GTG CGA AGG GTA GCG AT-3'

TEG: Tetra-Ethylene Glycol

Confocal microscope: The samples are imaged using a fast scanning confocal

microscope (Leica TCS SP5 II).

Light microscope with a temperature stage: A Leica DMRXA microscope with Qimaging Retiga 1300 camera is used to obtain microscopic images. A temperature stage is built on the light microscope to provide fast *in-situ* temperature control. Briefly, 1000 Ω ITO glass is placed on a 3mm thick copper plate, two ends of which are connected to peltiers (2.5cm by 2.5cm) then to a thermal sink with constant temperature. With LakeShore DRC 93C Temperature Controller and LakeShore PT-111 temperature sensor, we are able to control and detect the temperature with $<0.5^{o}C$ relative error.

Acknowledgements: We would like to thank Ruojie Sha and Nadrian Seeman for useful discussions and a careful reading of the manuscript. This work is supported partially by the MRSEC Program of the National Science Foundation under Grant No. DMR-0820341 and the National Science Foundation Career Grant No. 0955621.

Arthur Contributions:
L.F. and L.-L.P. designed and performed experiments, built the model, analyzed data and wrote the paper; R.D. designed experiments; P.C. and J.B. initiated and directed the project, designed experiments, analyzed data and wrote the paper.

References:

1. Seeman, N. C. DNA in a material world. *Nature* **421**, 427–431 (2003).
2. Alivisatos, A. P. *et al*. Organization of 'nanocrystal molecules' using DNA. *Nature* **382**, 609–611 (1996).
3. Mirkin, C. A., Letsinger, R. C., Mucic, R. C. & Storhoff, J. J. A DNA-based method for rationally assembling nanoparticles into macroscopic materials. *Nature* **382**, 607–609 (1996).
4. Macfarlane, R.J. *et al.* Nanoparticle Superlattice Engineering with DNA. *Science* **334**, 6053, 204-208 (2011).
5. Nykypanchuk, D., Maye, M. M., van der Lelie, D. & Gang, O. DNA-guided crystallization of colloidal nanoparticles. *Nature Mater.* **451**, 549–552 (2008).
6. Biancaniello, P. L., Kim, A. J. & Crocker, J. C. Colloidal interactions and self-assembly using DNA hybridization. *Phys. Rev. Lett.* **94**, 058302 (2005).
7. Kim, A. J., Biancaniello, P. L. & Crocker, J. C. Engineering DNA-mediated colloidal crystallization. *Langmuir* **22**, 1991–2001 (2006).
8. Zheng, J. *et al.* From Molecular to Macroscopic *via* the Rational Design of a Self-Assembled 3D DNA Crystal, *Nature* **461**, 74-77 (2009).
9. Wang, T. *et al*. Self-Replication of information-bearing nanoscale pattern. *Nature* **478**, 225-228 (2011).
10. Leunissen, M. E. *et al.* Towards self-replicating materials of DNA-functionalized colloids. *Soft Matter* **5**, 2422–2430 (2009).
11. Wang, Y. *et al*. Colloids with valence and specific directional binding. *Nature* **491**, 51-55 (2012)
12. Hadorn, M., *et al.* Specific and reversible DNA-directed self-assembly of oil-in-water emulsion droplets. *Proc. Natl Acad. Sci. USA* **109**, 20320–20325 (2012).
13. Lee, J., Hernandez, P., Lee, J., Govorov, A. O. & Kotov, N. A. Exciton–plasmon interactions in molecular spring assemblies of nanowires and wavelength-based protein detection. *Nature Mater.* **6**, 291–295 (2007) (plasmonic)
14. Feng, L. P., Park, S. H., Reif, J. H. & Yan, H. A two-state DNA lattice switched by DNA nanoactuator. *Angew. Chem. Int. Ed.* **42**, 4342–4346 (2003). (mechanical)
15. Redl, F. X., Cho, K. S., Murray, C. B. & O'Brien, S. Three-dimensional binary superlattices of magnetic nanocrystals and semiconductor quantum dots. *Nature* **423**, 968–971 (magnetical)
16. Urban, J. J., Talapin, D. V., Shevchenko, E. V., Kagan, C. R. & Murray, C. B. Synergism in binary nanocrystal superlattices leads to enhanced p-type conductivity in self-assembled PbTe/Ag-2 Te thin films. *Nature Mater.* **6**, 115–121 (2007) (electronical)
17. Valignat, M. P., Theodoly, O., Crocker, J. C., Russel, W. B. & Chaikin, P. M. Reversible self-assembly and directed assembly of DNA-linked micrometer-sized colloids. *Proc. Natl Acad. Sci. USA* **102**, 4225–4229 (2005).
18. Maye, M.M *et al.* Switching binary states of nanoparticle superlattices and dimer

clusters by DNA strands. *Nature Nanotech.* **5**, 116 - 120 (2010) (DNA nano-particles)
19. Pontani, L.-L., Jorjadze, I., Viasnoff, V. and Brujic, J. Biomimetic emulsions reveal the effect of mechanical forces on cell–cell adhesion *Proc. Natl Acad. Sci. USA* **109**, 9839-9844(2012).
20. Tkachenko, A.V. Theory of programmable hierarchic self-assembly. *Phys. Rev. Lett.* **106**, 255501 (2011)
21. Martinez-Veracoechea, F.J., Mladek, B.M., Tkachenko, A.V. and Frenkel, D. Design rule for colloidal crystal of DNA-functionalized particles. *Phys. Rev. Lett.* **107**, 045902 (2011)
22. Dreyfus, R. *et al*. Simple quantitative model for the reversible association of DNA coated colloids. *Phys. Rev. Lett.* **102**, 048301 (2009).
23. Dreyfus, R. *et al*. Aggregation-disaggregation transition of DNA coated colloids: experiments and theory *Phys. Rev. E*, **81**, 041404 (2010)
24. Angioletti-Uberti, S., Mognetti, B.M. and Frenkel, D. Re-entrant melting as a design principle for DNA-coated colloids. *Nature Materials* **11**, 518–522 (2012)
25. Jones, M.R. *et al*. DNA-nanoparticle superlattices formed from anisotropic building blocks. *Nature Mater.* **9**, 913–917 (2010).
26. M. C. Murphy, I. Rasnik, W. Cheng, T. M. Lohman, and T. Ha, Probing single-stranded DNA conformational flexibility using fluorescence spectroscopy. Biophys. J. 86, 2530 (2004).
27. Clegg, R.M. and Vaz, W.L.C., Translational diffusion of proteins and lipids in artificial lipid bilayer membranes. A comparison of experiment with theory, *Progress in Protein–Lipid Interactions*, **1**, 173–229 (1985)
28. Vaz, W.L.C., Clegg, R.M. and Hallmann, D., Translational diffusion of lipids in liquid crystalline phase phosphatidylcholine multibilayers. A comparison of experiment with theory, *Biochemistry*, **24**, 781-786, (1985)
29. Negishi, M., Seto, H., Hase, M. and Yoshikawa, K., How Does the Mobility of Phospholipid Molecules at a Water/Oil Interface Reflect the Viscosity of the Surrounding Oil? *Langmuir*, **24(16)**, 8431-8434, (2008)
30. Walder, R.B., Honciuc, A., Schwartz, D.K., 'Phospholipid diffusion at the oil-water interface', J.Phys.Chem.B. 2010, 114, 11484-11488.

Figure Legends

Figure 1:

Adhesive DNA-emulsion systems. (A) The silicone oil droplets are stabilized with

phospholipids, some of which are labeled with fluorescently dyed streptavidin that allow the grafting of S or S' DNA strands. The S functionalized emulsion is dyed in green while the S' one is dyed in red. The complementary S and S' sticky ends then bind and form adhesion patches enriched in DNA tethers between the droplets. (B) colloids coated with the S DNA strand and dyed in green can stick to S' functionalized droplets and eventually bridge to droplets together through a colloidal patch. (C) Below the DNA melting temperature T_m=50°C the complementary thermal droplets aggregate into clusters (left) that are disrupted above the T_m (right). (D) Similarly the S coated particles only stick to the complementary S' emulsion below T_m (left) to form large composite structures of multiple droplets linked through particles. Those clusters as well as individual droplet-particle interactions dissociate above T_m (right).

Figure 2:

Entropy-dependent adhesion patches between complementary emulsions.

Confocal imaging of S(green) and S'(red) complementary emulsions interaction reveals the formation of adhesion patches for double stranded (dsb) (A) and single stranded (ssb) (B) constructs. (C) Diameter of the patch as a function of the squared radius <R> for two interacting droplets of radii R_1 and R_2 for dsb (black squares) and ssb DNA (red circles), with $< R >= \sqrt{\frac{2R^2_1 R^2_2}{R^2_1 + R^2_2}}$. The data are fitted by the model (dashed lines). (D) The growth of the patch size (diameter/<R>) is plotted as a function of time for dsb (black squares) and ssb (red circles) DNA. Green triangles record the growth of ssb patches after addition of complementary strands, which turn into dsb patches after ~40min.

Figure 3: **The dependence of patch size and intensity on DNA coverage.**

(A) Confocal images of the adhesion patches between complementary droplets for increasing DNA coverages on the droplets surface (DNA coverage from left to right: (left) ~17% (middle) ~34% (right) 100% which is ~1400 strands/μm^2). The patch angle θ (B) and relative intensity (C) are plotted as a function of the relative DNA coverage on the droplets. The experimental data are well fitted by the model (solid lines).

Figure 4: **Diffusivity of complementary bonds.**

(A) Green emulsion droplet diffuses on a complementary droplet along with the adhesion patch. (B) Two S coated particles bound to a S' coated droplet diffuse on its surface. The mean square displacement of the particles with time reveals a diffusive behavior with a diffusion coefficient $D=0.012\mu m^2/s$ on the surface of phospholipid stabilized emulsions. (C) Emulsion network connected by specific DNA bonds.

Figure 5: Self-**assembly of the colloid-emulsion system.**

(A) Polymer chain of emulsion droplets stabilized by two adhesion patches formed using complementary nanoparticles. The divalent emulsion droplets result from a low nanoparticle/droplet ratio ~5.

(B) At higher nanoparticle/droplet ratios more than two adhesion patches can form, leading in this case to a trivalent 2D structure. (C) Large particle/droplet ratios, ~ 100, can produce multivalent droplets and lead to compact rigid structures in which the beads (green) all assemble between the droplets (red) contacts to minimize the system's energy. (D) The colloidal nanoparticles assemble as rings between droplets contacts to maximize the amount of droplet/particle adhesive area with little droplet deformation.

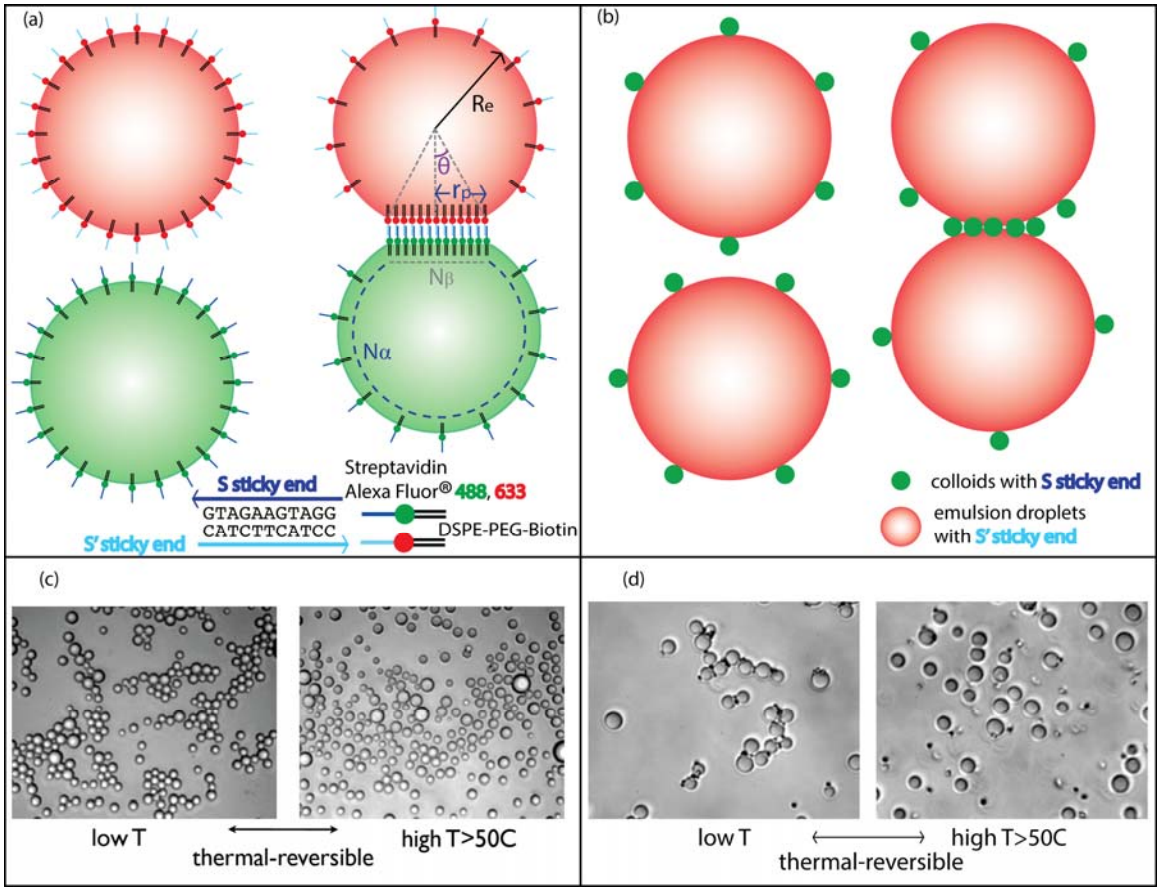
(a)
Re
θ
rp
Nβ
Nα
S sticky end
GTAGAAGTAGG
CATCTTCATCC
S' sticky end
Streptavidin
Alexa Fluor® 488, 633
DSPE-PEG-Biotin
(b)
colloids with S sticky end
emulsion droplets
with S' sticky end
(c)
low T
high T>50C
thermal-reversible
(d)
low T
high T>50C
thermal-reversible

Figure1

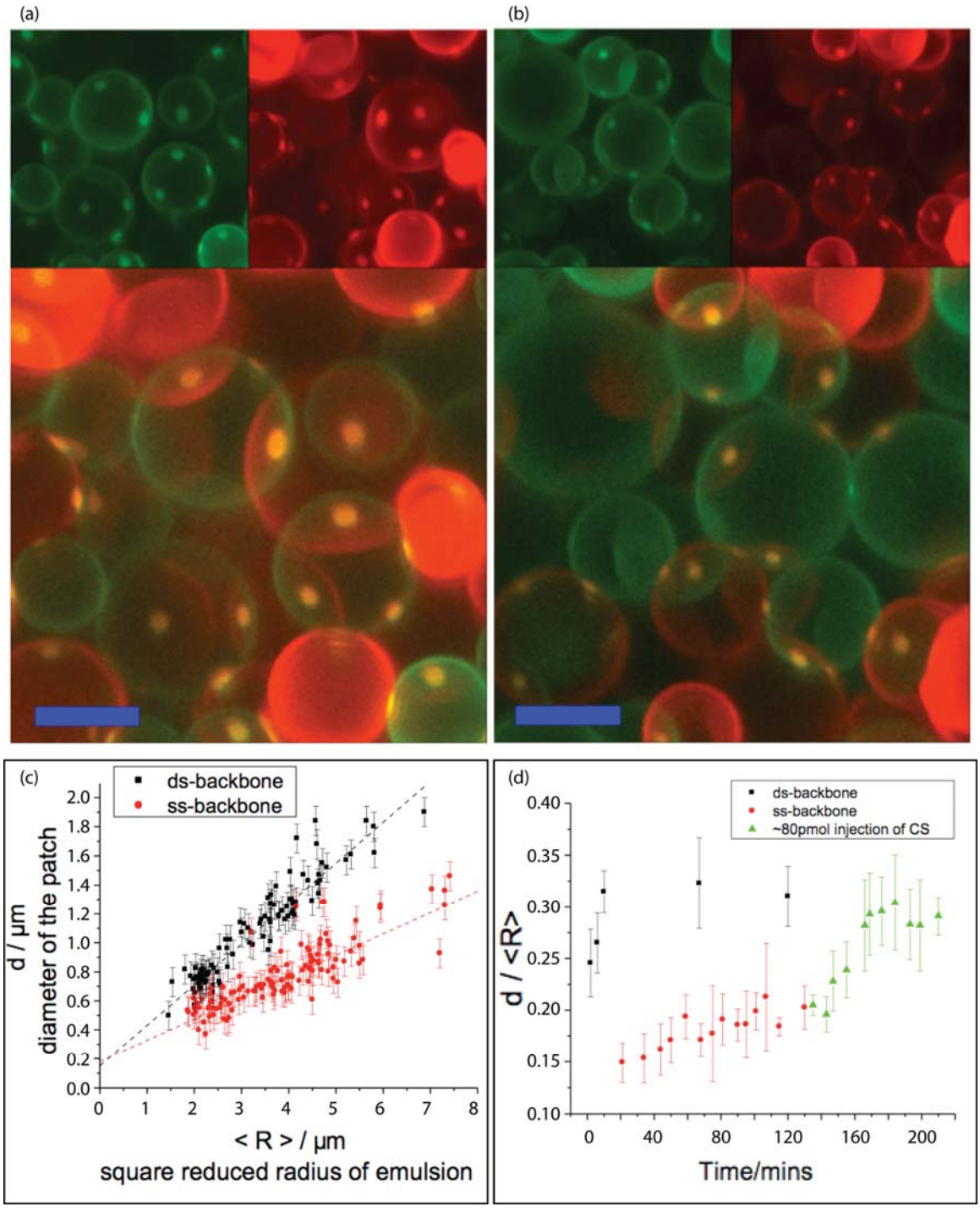
(a)
(b)
(c)
ds-backbone
ss-backbone
d / µm
diameter of the patch
< R > / µm
square reduced radius of emulsion
(d)
ds-backbone
ss-backbone
~80pmol injection of CS
d / <R>
Time/mins

Figure2

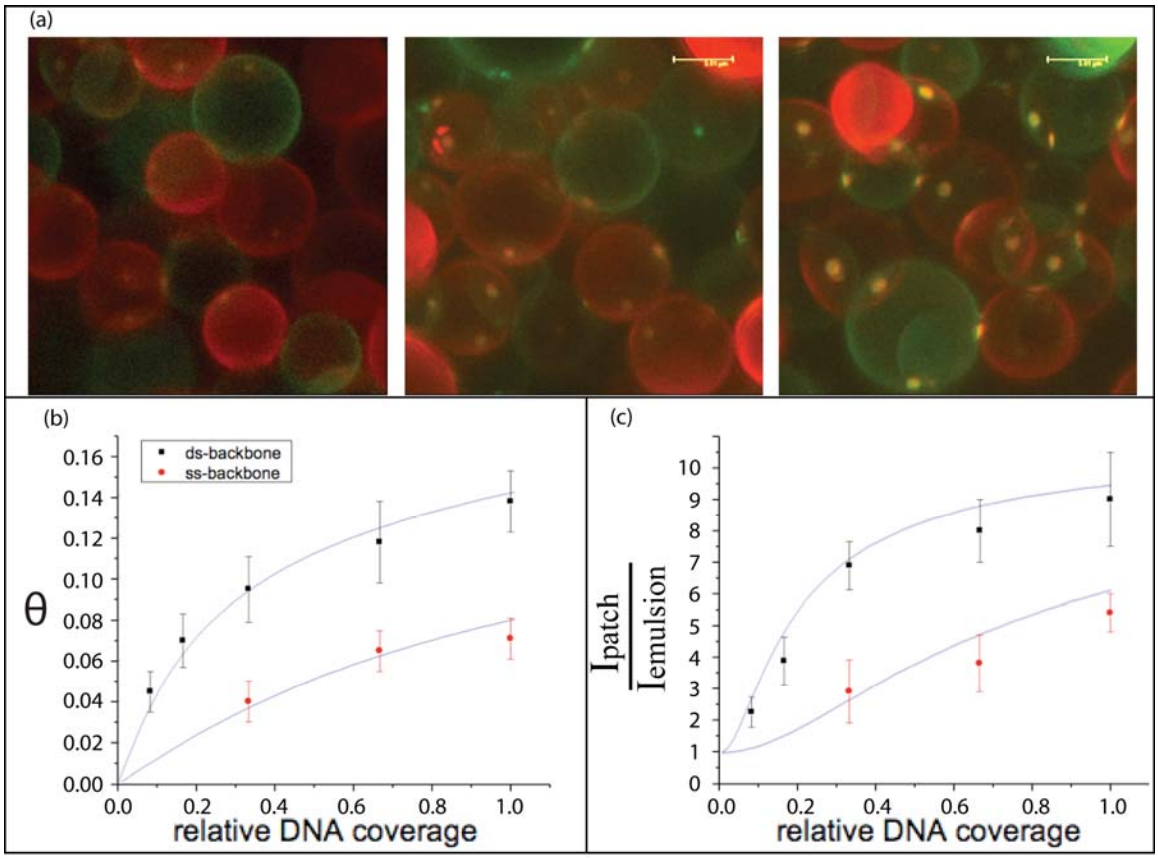
(a)
(b)
ds-backbone
ss-backbone
θ
0.16
0.14
0.12
0.10
0.08
0.06
0.04
0.02
0.00
0.0
0.2
0.4
0.6
0.8
1.0
relative DNA coverage
(c)
Ipatch / Iemulsion
10
9
8
7
6
5
4
3
2
1
0
0.0
0.2
0.4
0.6
0.8
1.0
relative DNA coverage

Figure3

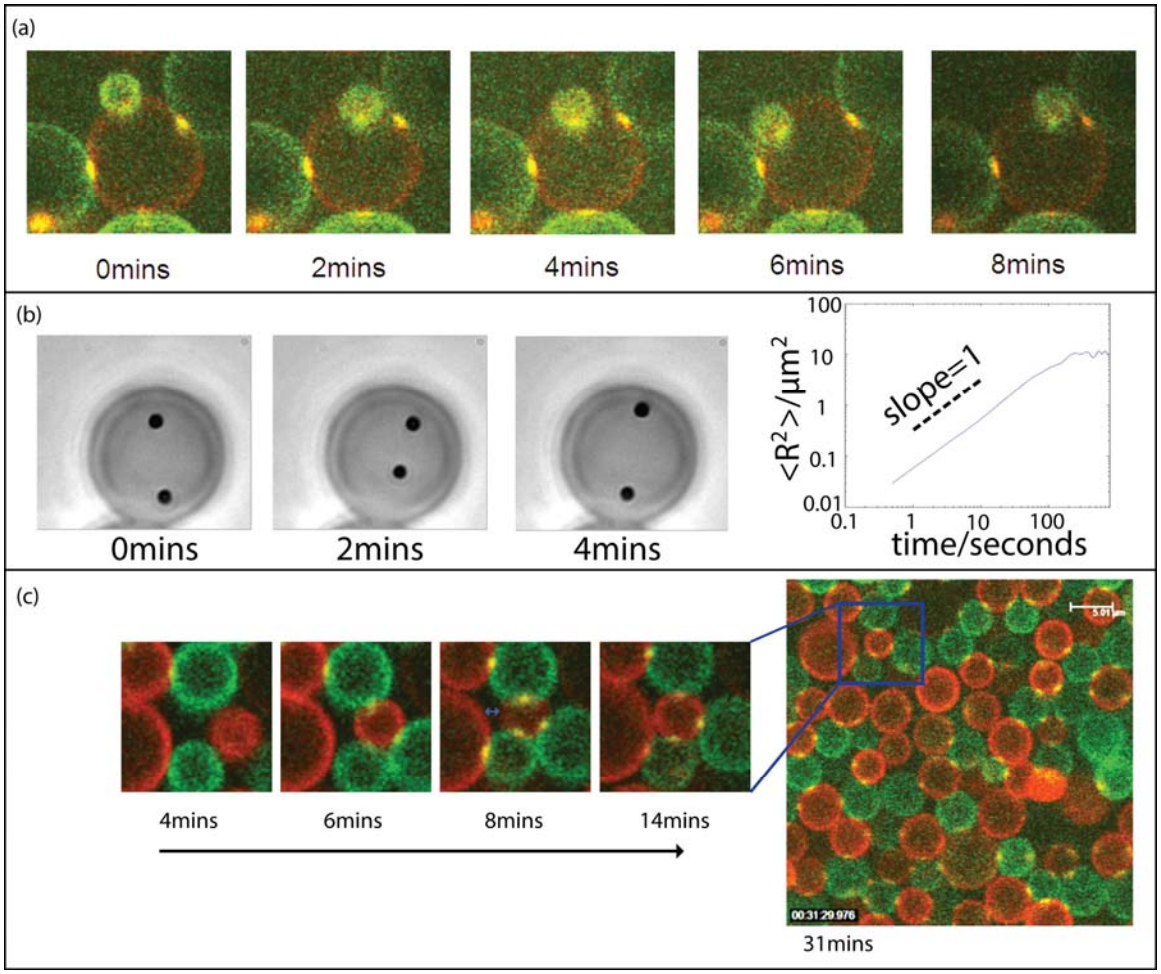
(a)
0mins
2mins
4mins
6mins
8mins
(b)
0mins
2mins
4mins
100
10
1
0.1
0.01
0.1
1
10
100
<R²>/μm²
slope=1
time/seconds
(c)
4mins
6mins
8mins
14mins
31mins

Figure4

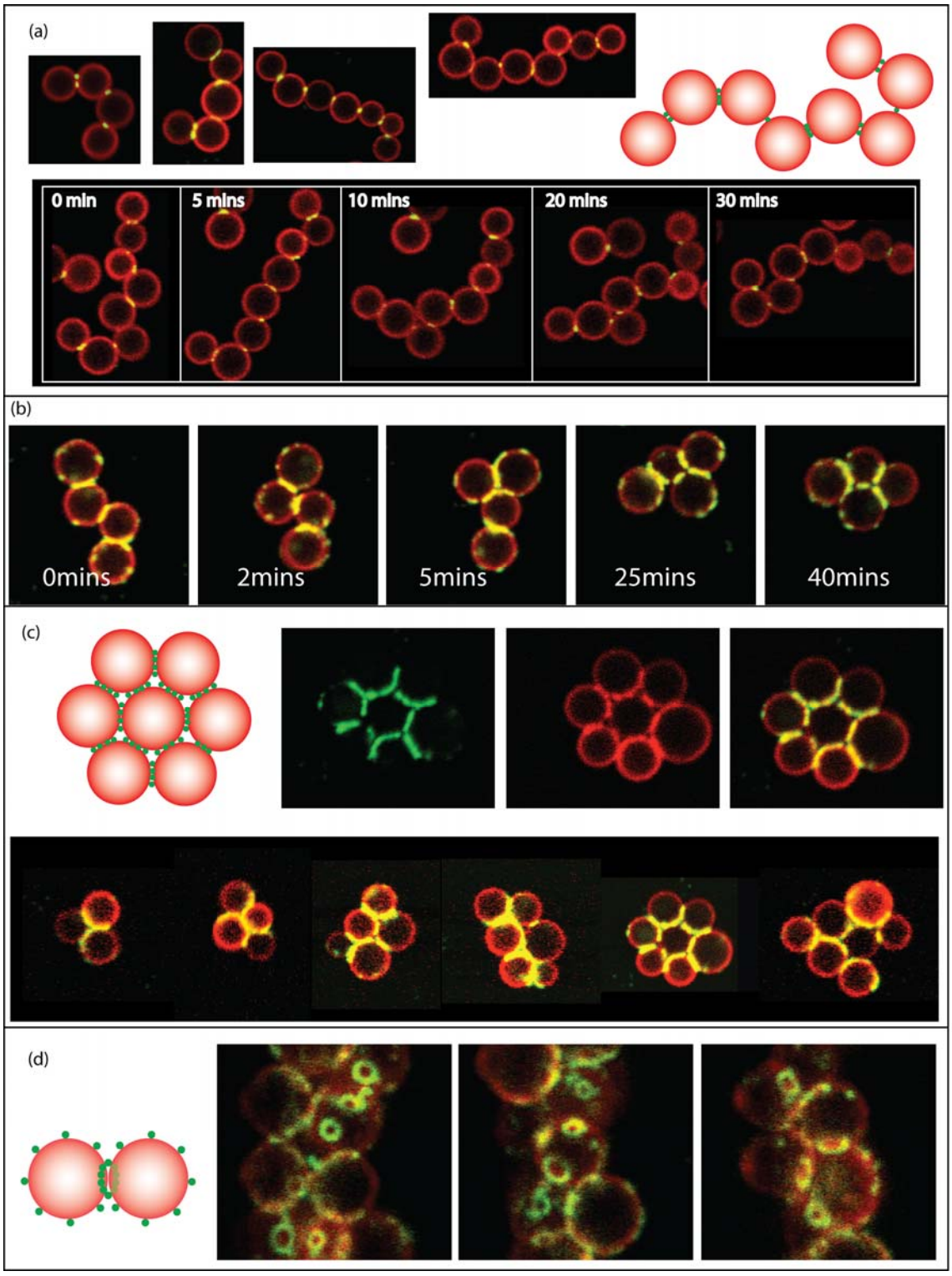
(a)
0 min
5 mins
10 mins
20 mins
30 mins
(b)
0mins
2mins
5mins
25mins
40mins
(c)
(d)

Figure5